Monthly Notices
of the
ROYAL ASTRONOMICAL SOCIETY

Mon. Not. R. Astron. Soc. **417,** 681–688 (2011) doi:10.1111/j.1365-2966.2011.19310.x

Cold accretion discs and lineless quasars

Ari Laor[1]★ and Shane W. Davis[2]★

[1]*Physics Department, Technion, Haifa 32 000, Israel*
[2]*Canadian Institute for Theoretical Astrophysics, Toronto, ON M5S 3H4, Canada*

Accepted 2011 June 23. Received 2011 June 22; in original form 2011 April 27

ABSTRACT

The optical–UV continuum of quasars is broadly consistent with the emission from a geometrically thin optically thick accretion disc (AD). The AD produces the ionizing continuum which powers the broad and narrow emission lines. The maximum AD effective temperature is given by $T_{\rm eff,max} = f_{\rm max}(\dot{M}/M^2)^{1/4}$, where M is the black hole mass, $\dot{M}$ the accretion rate and $f_{\rm max}$ is set by the black hole spin a_*. For a low enough value of $\dot{M}/M^2$, the AD may become too cold to produce ionizing photons. Such an object will form a lineless quasar. This occurs for a local blackbody (BB) AD with a luminosity $L_{\rm opt} = 10^{46}\,{\rm erg\,s^{-1}}$ for $M > 3.6 \times 10^9\,{\rm M_\odot}$, when $a_* = 0$, and for $M > 1.4 \times 10^{10}\,{\rm M_\odot}$, when $a_* = 0.998$. Using the AD-based $\dot{M}$, derived from M and $L_{\rm opt}$, and the reverberation-based M, derived from $L_{\rm opt}$ and the Hβ full width at half-maximum, v, gives $T_{\rm eff,max} \propto L_{\rm opt}^{-0.13} v^{-1.45}$. Thus, $T_{\rm eff,max}$ is mostly set by v. Quasars with a local BB AD become lineless for $v > 8000\,{\rm km\,s^{-1}}$, when $a_* = 0$, and for $v > 16\,000\,{\rm km\,s^{-1}}$, when $a_* = 0.998$. Higher values of v are required if the AD is hotter than a local BB. The AD becoming non-ionizing may explain why line-emitting quasars with $v > 10\,000\,{\rm km\,s^{-1}}$ are rare. Weak low-ionization lines may still be present if the X-ray continuum is luminous enough, and such objects may form a population of weak line quasars (WLQ). If correct, such WLQ should show a steeply falling spectral energy distribution (SED) at $\lambda < 1000$ Å. Such an SED was observed by Hryniewicz et al. in SDSS J094533.99+100950.1, a WLQ observed down to 570 Å, which is well modelled by a rather cold AD SED. UV spectroscopy of $z \sim 1$–2 quasars is required to eliminate potential intervening Lyman limit absorption by the intergalactic medium and to explore if the SEDs of lineless quasars and some additional WLQ are also well fitted by a cold AD SED.

Key words: accretion, accretion discs – black hole physics – galaxies: active – quasars: general.

1 INTRODUCTION

The optical–UV spectral energy distribution (SED) of quasars is broadly consistent with the expected emission of a thin accretion disc (AD) around a massive black hole (BH) (Shields 1978; Czerny & Elvis 1987; Sun & Malkan 1989; Laor 1990; Blaes et al. 2001; Shang et al. 2005). Various spectral features, such as the general turnover at $\lambda < 1000$ Å (Zheng et al. 1997; Telfer et al. 2002; Barger & Cowie 2010), the observed optical–UV spectral slopes (Bonning et al. 2007; Davis, Woo & Blaes 2007), the small dispersion in the UV/optical flux ratio (Davis & Laor 2011) and microlensing variability (Morgan et al. 2010; Blackburne et al. 2011), may imply various modifications beyond the simplest AD models (see review by Koratkar & Blaes 1999, and references therein). One should note that some of the expected AD spectral features may be diluted by various unrelated emission components (Kishimoto et al. 2004, 2008).

The peak of the simplest AD model of local blackbody (BB) emission occurs at $\nu_{\rm peak} \propto (\dot{M}/M^2)^{1/4}$ (see Section 2), or equivalently $\nu_{\rm peak} \propto (l/M)^{1/4}$, where M is the BH mass, $\dot{M}$ is the accretion rate and $l = L/L_{\rm Edd}$ is the ratio of the bolometric luminosity to the Eddington luminosity. Thus, when M increases from 10 to $10^9\,{\rm M_\odot}$, at a fixed l, the disc cools by a factor of 100. This factor is consistent with the drop from $\nu_{\rm peak} \simeq 1$–2 keV in X-ray binary systems (e.g. Remillard & McClintock 2006) to $\nu_{\rm peak} \simeq 10$–20 eV, observed in quasars. The quasar SED peaks at about the H ionization threshold, and thus provides ample ionizing luminosity which powers the broad and narrow line emission.

A further extrapolation of the expected AD SED to $M > 10^9\,{\rm M_\odot}$ and $l < 0.1$ leads to $\nu_{\rm peak} < 10$ eV and thus to a non-ionizing AD SED (see e.g. fig. 5 in Laor & Netzer 1989, for a model where

★E-mail: laor@physics.technion.ac.il (AL); swd@cita.utoronto.ca (SWD)

$\nu_{\rm peak} \simeq 1$–$2\,{\rm eV}$). Such models appeared inconsistent with the observations, as the SED of such quasars cannot power strong line emission. Such quasars will appear mostly as luminous continuum sources. Some line emission can still be produced through X-ray photoionization. However, in luminous quasars the fraction of the bolometric luminosity in the X-ray drops well below 10 per cent (Just et al. 2007), and the fraction of the bolometric power available for line emission thus drops from >50 to <10 per cent., i.e. by a factor of >5. The total line emission should drop by a similar factor.

Observational evidence that weak line quasars (WLQ) do exist started to accumulate since the discovery of McDowell et al. (1995) that in PG 1407+265 all lines, except Hα, are exceptionally weak. A BL Lac origin could be clearly excluded based on its SED which overlaps well the mean SED of optically selected quasars (Elvis et al. 1994). Additional WLQ were discovered in various other studies (Fan et al. 1999, 2006; Anderson et al. 2001; Hall et al. 2002, 2004; Reimers et al. 2005; Ganguly et al. 2007; Leighly et al. 2007a; Hryniewicz et al. 2010), and were followed up by dedicated studies of larger samples of WLQ at a range of wavelengths (Diamond-Stanic et al. 2009; Shemmer et al. 2009, 2010; Plotkin et al. 2010a,b; Wu et al. 2011). The observed radio to X-ray SEDs of most WLQ are consistent with the mean SED of radio-quiet quasars, and clearly excludes the BL Lac interpretation for the absence of line emission. Proposed explanations for WLQ invoked unusual broad-line region (BLR) properties, such as a low covering factor, an anisotropic ionizing source or BLR shielded from the ionizing source.

A possibly related issue is that of 'true type 2' active galactic nuclei (AGN), i.e. AGN which lack broad lines, but appear to be unobscured (Tran 2003; Shi et al. 2010). These objects differ from WLQ in two ways. First, they are defined by the lack of broad lines, and not by the lack of lines in general. However, once $z \gtrsim 1$, the significant narrow lines are redshifted from optical spectroscopy, and one cannot separate a lineless quasar from a type 2 AGN. Secondly, the 'true type 2' AGN tend to reside at $l < 10^{-2}$ (Shi et al. 2010; Trump et al. 2011), in contrast to WLQ which typically have $l \sim 0.1$–1 (e.g. Shemmer et al. 2010).

Various suggestions were made to explain the lack of broad lines in unobscured type 2 AGN. Nicastro (2000) and Nicastro, Martocchia & Matt (2003) suggested that the BLR is formed by AD instabilities occurring in a critical radius where the disc changes from gas pressure dominated to radiation pressure dominated. This critical radius can become smaller than the innermost stable orbit, and then the BLR cannot form. Czerny, Rózańska & Kuraszkiewicz (2004) and Elitzur & Ho (2009) suggested that the transition of the AD from a cold geometrically thin flow to a hot advection-dominated accretion flow eliminates the AD wind which launches the BLR. Elitzur & Shlosman (2006) suggested that the BLR is formed by a torus outflow, and below a certain accretion rate the outflow transforms into radio jets, and the BLR disappears. The various physical mechanisms suggested above to eliminate the BLR generally occur below some values of l, which may be a function of M. These ranges correspond to a certain maximum linewidth, which may be a function of L, beyond which all AGN become 'true type 2' AGN. Laor (2003) pointed out that the BLR appears not to be detectable at full width at half-maximum (FWHM) > $25\,000\,{\rm km\,s^{-1}}$, which may either be a detection limit or a maximal velocity where the BLR can exist. However, no physical mechanism was put forward to explain why the BLR FWHM may be the primary parameter for the existence of the BLR. As shown below, a non-ionizing AD may provide a simple explanation for the observed luminosity independent of upper limit on the BLR FWHM.

In the following section we derive the AD model parameters which produce a cold AD, i.e. an AD with a non-ionizing SED. In Section 3 we show that the SED of a WLQ, observed as far as 570 Å, is fitted surprisingly well by a cold AD model. In Section 4 we discuss additional implications, and the relevance to other observed properties of AGN. The main conclusions are summarized in Section 5.

2 NON-IONIZING AD MODEL PARAMETERS

Below we first derive the relation between $T_{\rm eff,max}$ and the AD model parameters, based on the standard Shakura & Sunyaev (1973, hereinafter SS73) thin disc model. The flux emitted per unit area is

$$F = \frac{3}{8\pi}\frac{G\dot{M}M}{R^3} f(R, M, a_*), \tag{1}$$

where R is the radius and $f(R, M, a_*)$ is a dimensionless factor set by the inner boundary condition and the relativistic effects (Novikov & Thorne 1973; Riffert & Herold 1995). It is convenient to use the dimensionless radius, $r \equiv R/R_{\rm g}$, where $R_{\rm g} \equiv GM/c^2$, which gives

$$F = \frac{3c^6}{8\pi G^2}\frac{\dot{M}}{M^2 r^3} f(r, a_*), \tag{2}$$

where $f(r, a_*) \lesssim 1$.

The local effective temperature is $T_{\rm eff} \equiv (F/\sigma)^{1/4}$, and it scales as

$$T_{\rm eff} = T_0 f(r, a_*)^{1/4} r^{-3/4}, \tag{3}$$

where

$$T_0 \equiv \left(\frac{3c^6}{8\pi G^2 \sigma}\right)^{1/4} \frac{\dot{M}^{1/4}}{M^{1/2}}, \tag{4}$$

or in more convenient units

$$T_0 = 8.6 \times 10^5 \dot{M}_1{}^{1/4} m_8^{-1/2}\,{\rm K}, \tag{5}$$

where

$$\dot{M} = \dot{M}_1\,{\rm M_\odot\ yr^{-1}},$$

and

$$M = 10^8 m_8\,{\rm M_\odot},$$

or in cgs units

$$\dot{M} = 6.3 \times 10^{25} \dot{M}_1\,{\rm g\,s^{-1}},$$

and

$$M = 1.989 \times 10^{41} m_8\,{\rm g}.$$

We denote by $f_{\rm max}$ the maximum value of $f(r, a_*)$, which sets the maximum disc temperature $T_{\rm eff,max}$, assuming a local BB emission. The ratio $T_{\rm eff,max}/T_0$ is then a function of a_* only. Ratios for representative values of a_* are provided in Table 1. As a_* increases, the innermost marginally stable disc radius $r_{\rm ms}$ decreases, and $T_{\rm eff,max}/T_0$ increases.

Note that $f_{\rm max}$ is only a function of a_* as we have assumed the standard AD structure, where the viscous torque increases inwards, reaches a maximum, and then drops until it vanishes at the innermost stable circular orbit (ISCO). In reality, there is likely to be some magnetic stress at or near the inner boundary and continuing emission inside the ISCO. Quantifying the level of additional emission from near or inside the ISCO is an active research topic (e.g. Kulkarni et al. 2011; Noble et al. 2011). However, any additional emission is not likely to cause significantly greater variation in $f_{\rm max}$ than varying a_* alone. For example, Noble et al. (2011) generally argue for a larger effect due to emission inside the ISCO

Table 1. The results for local BB AD models, observed at $\mu = 0.8$. All the results in the table are independent of the values of m_8 and $\dot{M}_1$.

a_*	$T_{\rm eff,max}/T_0$	$h\nu_{\rm max}/kT_{\rm eff,max}$	$\nu_{0.1}/\nu_{\rm max}$	$\nu_{0.01}/\nu_{\rm max}$	$\nu_{\rm max}(\mu=0.8)/\nu_{\rm max}(\mu=0.3)$	A_μ
0	0.1	2.18	1.91	3.43	0.85	1.17
0.9	0.23	1.77	1.97	3.54	0.64	1.59
0.998	0.45	1.18	2.03	3.54	0.46	2.03

than Kulkarni et al. (2011). But they find that an $a_* = 0$ would appear as an $a_* = 0.2$–0.3 model if the emission at the disc surface is locally everywhere a BB. (Note, however, that the radiation inside the ISCO may be far from thermodynamic equilibrium due to the drop in disc surface density, so local BB emission may not be a good approximation there.) Hence, in this work we will focus on the simple AD models where $f_{\rm max}$ is determined solely by a_*.

What is the frequency $\nu_{\rm max}$ where the AD νL_ν peaks? For a single-temperature BB, it is simple to show that the peak occurs at $h\nu_{\rm max}/kT_{\rm max} = 3.92$. A local BB AD is a superposition of BBs with $T \le T_{\rm max}$, weighted by the emitting surface area and convolved by the relativistic effects. This superposition results in an integrated spectrum with a broader SED compared to a single-temperature BB, which peaks at $h\nu_{\rm max}/kT_{\rm max} < 3.92$. Table 1 lists the values of $h\nu_{\rm max}/kT_{\rm max}$, corresponding to an AD observed at $\mu \equiv \cos\theta = 0.8$, where θ is the inclination angle of the AD to the line of sight ($\mu = 1$ is face-on).

How low should $\nu_{\rm max}$ be for an AD to be called non-ionizing? Let us define a non-ionizing AD, or a cold AD, as an AD where the ionizing luminosity is $\le$0.01 of the bolometric luminosity. We now look for $\nu_{0.01}$, the frequency above which the integrated luminosity is 1 per cent of the bolometric luminosity, i.e.

$$\int_{\nu_{0.01}}^{\infty} L_\nu \, {\rm d}\nu \Big/ \int_0^{\infty} L_\nu \, {\rm d}\nu = 0.01.$$

If $\nu_{0.01} < 3.29 \times 10^{15}$ Hz, then the AD is cold. The values of $\nu_{0.01}\nu_{\rm max}$ depend on the AD SED, which is set by a_*. Table 1 provides $\nu_{0.01}/\nu_{\rm max}$ values for different a_* values, which all cluster at $\sim$3.5. Thus, a non-ionizing AD peaks at $\nu_{\rm max} < 9.4 \times 10^{14}$ Hz, or $\lambda_{\rm max} > 3200$ Å. Since the typical X-ray luminosity observed is $L_{\rm x} \lesssim 0.1 L_{\rm bol}$, the ionizing luminosity of a cold AD is $\sim$10 smaller than $L_{\rm x}$, and the ionization will be essentially all from $L_{\rm x}$.

We can also define a weakly ionizing AD as an AD where the ionizing luminosity is $\le 0.1 L_{\rm bol}$. For such an AD the AD ionizing luminosity is $\simeq L_{\rm x}$. Such objects will form a transition from UV-dominated ionization to X-ray-dominated ionization. Table 1 lists the values of $\nu_{0.1}/\nu_{\rm max}$, which cluster at $\sim$2. Setting $\nu_{0.1} < 3.29 \times 10^{15}$ Hz for a weakly ionizing AD implies that in such an AD $\nu_{\rm max} < 1.65 \times 10^{15}$ Hz, or $\lambda_{\rm max} > 1800$ Å.

Using the calculated values of $\nu_{0.01}/\nu_{\rm max}$, $h\nu_{\rm max}/kT_{\rm eff,max}$ and $T_{\rm eff,max}/T_0$, for a given a_*, as provided in Table 1, we derive the following upper limits for a cold AD:

$$T_0 \le 2.08 \times 10^5 \, {\rm K},$$

for $a_* = 0$, and

$$T_0 \le 7.98 \times 10^4 \, {\rm K},$$

for $a_* = 0.998$. Inserting these limits into equation (5) yields the conditions

$$\dot{M}_1 < 3.42 \times 10^{-3} m_8^2, \quad (6)$$

when $a_* = 0$, and

$$\dot{M}_1 < 7.41 \times 10^{-5} m_8^2, \quad (7)$$

when $a_* = 0.998$. If m_8 is known, then $\dot{M}_1$ can be estimated from the AD model fit to the optical (5100 Å) luminosity, $L_{\rm opt}$. Using equation (8) in Davis & Laor (2011),[1]

$$\dot{M}_1 = 3.5 m_8^{-0.89} L_{\rm opt,45}^{1.5}, \quad (8)$$

where $L_{\rm opt,45} = L_{\rm opt}/10^{45}$, we obtain the lower limits on $L_{\rm opt}$, below which the AD is cold:

$$L_{\rm opt,45} < 9.85 \times 10^{-3} m_8^{1.93}, \quad (9)$$

for $a_* = 0$, and

$$L_{\rm opt,45} < 7.66 \times 10^{-4} m_8^{1.93}, \quad (10)$$

for $a_* = 0.998$. Thus, even luminous quasars can become lineless, if m_8 is high enough. For example, for $L_{\rm opt} = 10^{46}$ erg s^{-1}, the AD becomes too cold to ionize when $M > 3.6 \times 10^9$ M$_\odot$ for $a_* = 0$, or for $M > 1.4 \times 10^{10}$ M$_\odot$ for $a_* = 0.998$. The corresponding values for l are $\lesssim$0.22 and $\lesssim$0.06, using the approximation $L_{\rm bol} \simeq 10 L_{\rm opt}$, i.e. $L_{\rm bol} = 10^{47}$ erg s^{-1}, and the implied relation $l = L_{\rm opt,45}/1.25 m_8$. Low-luminosity AGN need to have lower l values to have a cold AD. For example, AGN at $L_{\rm opt} = 10^{42}$ erg s^{-1} need to have $l \lesssim 2.6 \times 10^{-3}$ when $a_* = 0$ and $l \lesssim 7 \times 10^{-4}$ when $a_* = 0.998$ to become cold.

The value of M is commonly estimated using the broad emission lines. Kaspi et al. (2000) gives

$$m_8 = 1.5 L_{\rm opt,45}^{0.69} v_{3000}^2, \quad (11)$$

where $v_{3000} = {\rm H}\beta$ FWHM/3000 km s^{-1}. Inserting the Kaspi et al. relation to equation (8) above gives (Davis & Laor 2011, equation 9)

$$\dot{M}_1 = 2.5 L_{\rm opt,45}^{0.87} v_{3000}^{-1.78}. \quad (12)$$

Inserting these two expressions to equations (6) and (7) yields

$$v_{3000} \ge 2.72 L_{\rm opt,45}^{-0.088}, \quad (13)$$

when $a_* = 0$, and

$$v_{3000} \ge 5.28 L_{\rm opt,45}^{-0.088}, \quad (14)$$

when $a_* = 0.998$. Thus, the criterion for a non-ionizing AD is set almost purely by the value of the Hβ FWHM, and is very weakly dependent on $L_{\rm opt}$. The AD becomes cold for Hβ FWHM $>$ 8160 km s^{-1}, when $a_* = 0$, or for Hβ FWHM $>$ 15 840 km s^{-1}, when $a_* = 0.998$. The quasar may become lineless when the Hβ FWHM is above these limits. These maximal values for the Hβ FWHM for an ionizing AD may correspond to the maximum values of the observable Hβ FWHM, as quasars with broader lines may drop out from quasar surveys which are based on emission-lines selection, due to their significantly weaker line emission.

[1] Note that there is an error in the numerical factors in equations (5) and (7) of Davis & Laor (2011). The numerical factor in equation (5) should be $40/\pi^2(6hG^2/5c^2)^{1/3}$ rather than $160/\pi^3(6\pi^2 hG^2c^2/5)^{1/3}$. The numerical factor in equation (7) should be 1.4 M$_\odot$ yr^{-1} rather than 2.6 M$_\odot$ yr^{-1}. However, the fitting function for $\dot{M}$ in their equation (8), which corresponds to our equation (8), is unaffected.

Fig. 1 shows the range of SEDs for various AD models. All models have the same absolute accretion rate $\dot{M}_1 = 1$ and $\mu = 0.8$. The upper two panels show local BB AD models. In both panels the SED gets softer as M increases, since $\nu_{\max} \propto M^{-1/2}$ (see equation 4). At a given M, the SED is softer for the $a_* = 0$ model, and $\nu_{\max}$ is a factor of 2.4 lower compared to the $a_* = 0.998$ model (as can be deduced from Table 1). Note that although the $a_* = 0.998$ AD is hotter than the $a_* = 0$ case by a factor of $T_{\rm eff,max}(a_* = 0.998)/T_{\rm eff,max}(a_* = 0) = 4.5$, the SED of the $a_* = 0$ model has $h\nu_{\max}/kT_{\rm eff,max} = 2.18$ compared to only 1.18 for the $a_* = 0.998$ model, which makes the $a_* = 0.998$ model $\nu_{\max}$ only a factor of 2.4 higher than for the $a_* = 0$ model. Each curve is labelled with the ionization fraction $f_{\rm ion}$, which is defined as the fraction of the bolometric luminosity that is radiated at all wavelengths shortward of the Lyman edge.

There are two effects which can make the observed spectrum harder than shown in Fig. 1 for the local BB models. These effects will increase the required minimal Hβ FWHM for an AD to become cold. First, the AD SED is non-isotropic. In the Newtonian case only the normalization of the AD luminosity changes with inclination. However, the relativistic effects change also the shape of the SED, making it harder closer to an edge-on view. The BLR must subtend an appreciable fraction of the sky, as seen by the ionizing source. The BLR is most likely in the form of a thick torus-like configuration, coplanar with the AD. The ionizing SED seen by the BLR will then be harder than the observed SED, which is likely seen at a smaller inclination, closer to a face-on view. Assuming that the torus-like configuration, where the BLR resides, is restricted to $\mu < 0.5$, and the clear line-of-sight cone where the AGN is unobscured is restricted to $\mu > 0.5$, it is plausible to assume that the mean inclination of the BLR is $\mu = 0.3$, while our line of sight has a mean value of $\mu = 0.8$. Table 1 provides $\nu_{\max}(\mu = 0.8)/\nu_{\max}(\mu = 0.3)$, and shows that the BLR can be exposed to an SED a factor of 1.2–2.2 harder than the observed SED. If we denote $x_{0.01} = h\nu_{0.01}/kT_{\rm eff,max}$, and use the parameter $A_\mu = x_{0.01}(\mu = 0.3)/x_{0.01}(\mu = 0.8)$, then the minimal value for v_{3000} derived in equations (13) and (14) scales as $A_\mu^{0.69}$. Table 1 lists A_μ values for a range of a_* values. Applying this inclination correction for the hardness of the ionizing SED implies minimal Hβ FWHM values of 9090 ($a_* = 0$) and 25 820 km s^{-1} ($a_* = 0.998$).

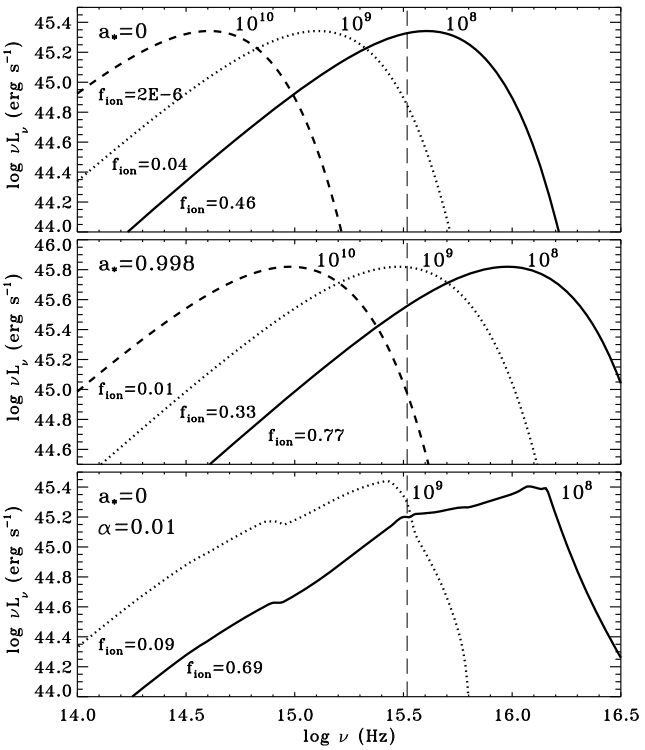

Figure 1. The SED of various AD models. All models have $\dot{M}_1 = 1$ and $\mu = 0.8$. The vertical dashed line shows the threshold ν for ionizing H. The two upper panels show various local BB AD models for $a_* = 0$ and $a_* = 0.998$. The SED gets softer as M increases and as a_* decreases. The lower panel shows the TLUSTY model (Hubeny et al. 2000) with $\alpha = 0.01$. The SED is harder than the local BB model, and the effect is larger when $T_{\rm eff,max}$ is larger. The fraction of ionizing radiation, $f_{\rm ion}$, is raised by the atmospheric effects, compared to the local BB AD models.

The second effect which can make the AD SED harder is deviations from the local BB approximation. A deviation from a local BB necessarily leads to a photospheric temperature $T > T_{\rm eff}$. Table 2 provides the ratios of $\nu_{\max}/T_{\rm eff,max}$ derived from detailed AD atmosphere models computed with TLUSTY. These model are physically equivalent to those presented in Hubeny et al. (2000), but utilize the interpolation scheme described in Davis & Hubeny (2006). Since we have a limited range of converged annuli, we only consider TLUSTY models with $a_* \leq 0.9$. In the local BB AD models $\nu_{\max}/T_{\rm eff,max}$ depends only on a_* and μ, as M and $\dot{M}$ only shift the SED, and do not affect its shape. In the atmospheric model the local emission is set by the photospheric density and temperature, and Table 2 provides models for the AD parameters which produce a relatively cold AD, relevant for our study. Since $T > T_{\rm eff}$ the SED is expected to be hotter compared to the BB model for the same parameters, and thus produce a higher $x_{0.01}$ value. A notable caveat is that some models have a strong Lyman absorption edge, which can lead to a lower $f_{\rm ion}$ compared to the local BB AD model, despite the higher T.

Fig. 1, lower panel, presents the AD SED derived from the TLUSTY models. The deviations of these detailed calculations from the simple BB approximation are strongly dependent on the local disc $T_{\rm eff,max}$ and the photospheric density. The photospheric density also depends (albeit more weakly) on the stress prescription, which is parametrized here using $\alpha = 0.01$ (SS73). The SS73 model gives a vertically averaged density which scales as α^{-1} in the radiation-dominated regime. The dependence of the photospheric density on α in TLUSTY models is typically much weaker, for reasons discussed in the appendix of Davis, Done & Blaes (2006), unless α and $\dot{M}$ are both large enough that the disc begins to become effectively optically thin. The SED can be significantly harder than the local BB model when $T_{\rm eff,max}$ is high. For example, $\nu_{\max}$ increases by a factor of $\sim$5 for the $m_8 = 1$, $\dot{M}_1 = 1$ model. However, the significantly colder ADs, which are of interest here, are not far from

Table 2. The TLUSTY model results, observed at $\mu = 0.8$. All models have a fixed $m_8 \times \dot{M}_1 = 1$, and therefore a fixed T_0. For the BB model, $h\nu_{0.1}/kT_{\rm eff,max} = 4.2$–$3.5$, and $h\nu_{0.01}/kT_{\rm eff,max} = 7.5$–$6.3$, for $a_* = 0$–0.9. In contrast to the BB case, we do not compute $a_* = 0.998$ models because our TLUSTY model atmosphere table is not extensive enough to reliably compute disc spectra for such high spins.

a_*	m_8	$\dot{M}_1$	$h\nu_{0.1}/kT_{\rm eff,max}$	$h\nu_{0.01}/kT_{\rm eff,max}$	$A_{\rm model}$
0	10	1.22	6.1	9.9	1.32
0	32	12.2	6.8	11.6	1.56
0	100	123	7.2	16.0	2.15
0.9	10	0.28	6.6	12.1	1.93
0.9	32	2.84	8.3	14.5	2.32
0.9	100	28.4	8.9	16.6	2.67

the local BB approximation. Table 2 provides the correction factors $A_{\rm model} = x_{0.01}({\rm TLUSTY})/x_{0.01}({\rm BB})$ for $\mu = 0.8$. Since $v_{3000} \propto A^{0.69}$, atmospheric effects can increase the minimal Hβ FWHM values by a factor of $\sim$1.2–2.

3 OBSERVATIONS

The SED of quasars with a cold AD should show a sharp cut-off beyond the Lyman limit. The WLQ population comes closest to the lineless quasars population. The WLQ with the highest rest-frame UV energy probed is SDSS J094533.99+100950.1, at $z = 1.66$, discovered by Hryniewicz et al. (2010). The *GALEX* far-UV (FUV) photometry extends down to rest frame 570 Å. Fig. 2 presents a local BB AD match to the overall SED presented by Hryniewicz et al. The AD model parameters were $m_8 = 27$ as estimated by Hryniewicz et al. based on the Mg II FWHM and the 3000 Å continuum luminosity. We assume an AD with a face-on view ($\mu = 1$). The value of $\dot{M}$ was then adapted to reproduce the overall SED normalization. The remaining free parameter is a_*, which is varied to match the FUV turnover. A suitable match to the data is found with $\dot{M}_1 = 11.4$ and $a_* = 0.3$. A good match can also be obtained with a higher inclination AD model, where the resulting harder SED is compensated by allowing a lower a_*. A reasonable match can be obtained down to $\mu = 0.6$, and $a_* = -1$, i.e. a BH counter-rotating with respect to the AD. A higher inclination, $\mu < 0.6$, is excluded, as the AD SED becomes too hard, and a_* cannot be further reduced to compensate for that. Similarly, a value of $a_* > 0.3$ is excluded, as the AD is too hard and μ cannot be further increased to compensate for that. These results are similar to those obtained by Czerny et al. (2011), who also discuss the effects of intrinsic reddening on the derived AD parameters. We also attempted TLUSTY model fits to the data; however, the SED of these models is broader than the local BB AD models, and a fit of comparable quality to the local BB AD models fit could not be obtained.

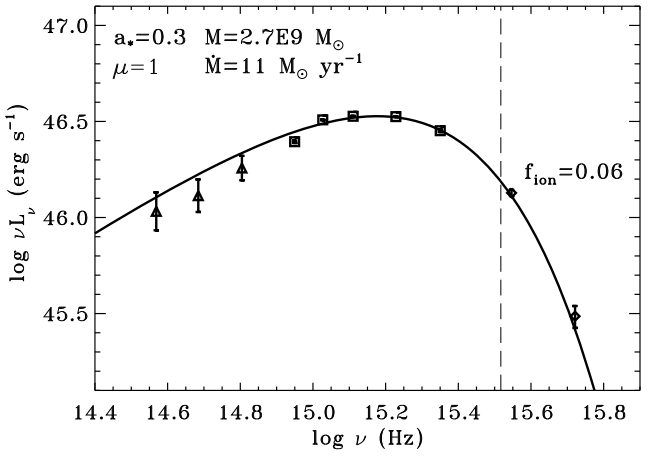

Figure 2. A local BB AD model match to the $z = 1.66$ weak emission-line quasar SDSS J094533.99+100950.1 from Hryniewicz et al. (2010). The TLUSTY models produced a lower quality match to the data. The photometric data points are taken from non-simultaneous observations by Two Micron All Sky Survey (triangles), SDSS (squares) and *GALEX* (diamonds). The AD model fit parameters are listed. The value of M is taken from Hryniewicz et al. The model peak position is mostly set by the combination of μ and a_*, and the normalization mostly by $\dot{M}$. The AD model fit gives $f_{\rm ion} = 0.06$, above our definition of $f_{\rm ion} = 0.01$ for potentially lineless quasar, and this higher value may be driving the weak low-ionization line emission observed.

Could the observed UV emission be significantly affected by the foreground Lyman forest absorption? Barger & Cowie (2010, their fig. 6) show that the cumulative effect of the Lyman α absorption systems along the line of sight suppresses the continuum at rest frame $912 < \lambda < 1216$ Å by a level of 4 per cent for $z = 1.1$. Using the evolution of the Lyman forest systems, $dn/dz \propto (1+z)^{2.23\pm1.2}$ for $0.9 < z < 1.7$ (Janknecht, Baade & Reimers 2002), the expected continuum suppression at $z = 1.66$ is <11 per cent, and is thus not significant. However, Lyman limit systems can produce significant absorption at rest frame $\lambda < 912$ Å. To affect the observed SED the Lyman limit absorber should occur longward of observed 1516 Å (the *GALEX* FUV effective wavelength), i.e. have $z > 0.66$. Using the number density per unit redshift evolution of $dn/dz = 0.15 \times (1+z)^{1.9}$ (Songaila & Cowie 2010), the expected number of absorbers integrated over $0.66 < z < 1.66$ is 0.66. A Lyman limit absorber will likely cause a break in the spectral curvature, which is not seen in the data (Fig. 2). A further complication may arise if a foreground Lyman break is diluted by a Lyman continuum emission edge produced by the AD. UV spectroscopy is required to clearly exclude foreground absorption effects on the observed FUV SED of SDSS J094533.99+100950.1.

4 DISCUSSION

The clear prediction of local BB AD models is that AGN with the correct combination of M and l harbour a luminous, but non-ionizing, continuum source. The UV SED of an AGN with $f_{\rm ion} = 0.01$ will show a peak at $\lambda > 3200$ Å, and a steep drop at $\lambda < 1000$ Å, and may form a lineless quasar, depending on the relative strength of the X-ray ionizing power-law continuum. An AGN with $f_{\rm ion} = 0.1$ will show a peak at $\lambda > 1800$ Å, and will likely form a WLQ, with an SED similar to that observed in the WLQ SDSS J094533.99+100950.1.

A cold non-ionizing AD is expected in luminous, $L_{\rm bol} \gtrsim 10^{47}\,{\rm erg\,s^{-1}}$, quasars even at relatively high values of $l \lesssim 0.2$, in particular for $a_* \simeq 0$. In low-luminosity AGN, $L_{\rm bol} \lesssim 10^{43}\,{\rm erg\,s^{-1}}$, the SED is predicted to become non-ionizing only at very low values of $l \lesssim 10^{-3}$. Since the X-ray/optical luminosity ratio is observed to increase with decreasing $L_{\rm bol}$, such low-luminosity and low-l AGN may be characterized by more prominent line emission, excited by the relatively stronger X-ray power-law emission.

What is the nature of the expected BLR emission? The flat X-ray power-law continuum produces an extended region of low ionization in the BLR gas, which is expected to cool mostly through collisionally excited low-ionization lines, such as Fe II and Mg II, and Balmer lines (collisionally excited due to highly trapped Lyα photons). The narrow-line region gas is expected to cool mostly through forbidden low-ionization lines, such as O I, N II and S II lines, as seen in low-ionization nuclear emission regions (LINERs; see photoionization model results in Ferland & Netzer 1983).

4.1 Are we missing lineless quasars?

Is it possible that AGN surveys are missing a significant number of moderately high-l, high-M AGN which are lineless? This can be addressed by surveys of AGN based on colour, independent of line emission. This was carried out by Diamond-Stanic et al. (2009) using the Slaon Digital Sky Survey (SDSS) sample, where they defined WLQ as having a Lyα EW < 15.4 Å, which is 3σ from the mean Lyα EW = 63.6 Å. They find that the fraction of quasars classified as WLQ increases from 1.3 per cent at $z < 4.2$ to 6.2 per cent at $z > 4.2$. Thus, lineless quasars do not form a significant part

of the quasar population, as expected given the required very high M values in luminous AGN, in order to have a cold AD.

4.2 Do LINERs have a cold AD?

In contrast to luminous AGN, a significant fraction of low-luminosity AGN near the more massive BH should fall in the cold AD regime. Theoretically, it is not clear whether the thin AD configuration remains valid at $l \lesssim 10^{-2}$, or whether the accretion transforms to an optically thin and geometrically thick configuration, which may produce a hard power-law continuum source (e.g. Narayan, Mahadevan & Quataert 1998). Observationally, the narrow emission lines of low-luminosity AGN in massive galaxies are generally characterized as LINERs, and are likely to be powered by a hard continuum source (Ferland & Netzer 1983), as their observed SED apparently suggests (e.g. Ho 2008; Eracleous, Hwang & Flohic 2010a; cf. Maoz 2007). Thus, the significant contribution of X-ray heating in low-luminosity AGN, given their flat α_{ox}, may imply that FUV heating is not significant in these objects anyhow, and its absence as the AD becomes cold will not affect their line emission significantly, unlike typical luminous AGN where the FUV dominates the line excitation. The line emission in LINERs may also be powered by additional mechanisms (e.g. Eracleous, Hwang & Flohic 2010b), which further lowers the diagnostic power of the line emission on the ionizing SED shape.

Interestingly, Lawrence (2005) finds that the change in the SED of a few potentially characteristic AGN, extending over a range of 10^6 in luminosity, is consistent with the expected change for an optically thick AD at a fixed M. It remains to be explored whether the optical–UV SED in the lowest luminosity AGN (e.g. LINER) can be fitted by a cold AD, or whether only a featureless hard power law is required. A cold AD in low-luminosity AGN cannot produce a lineless AGN, unless α_{ox} is unusually steep and ionizing radiation is indeed missing.

4.3 True type 2 AGN

In 'true type 2 AGN' which show normal (non-LINER) narrow lines, the absence of broad lines does not result from a cold AD, as an apparently normal photoionizing radiation, which excites the narrow lines, is present. In such objects, the BLR may be absent due to the absence of the mechanism which produces it, such as an AD wind, as proposed by Nicastro (2000), Nicastro et al. (2003), Czerny et al.(2004), Elitzur & Shlosman (2006) and Elitzur & Ho (2009).

4.4 What produces WLQ?

Are most WLQ powered by a cold AD? The archetype WLQ, PG 1407+265, is probably not, as its optical–UV SED appears to be similar to the average quasar SED (McDowell et al. 1995). It does not show the expected peak at $\lambda > 1800$ Å and a sharp drop at $\lambda < 1000$ Å (although the signal-to-noise ratio at $\lambda < 1000$ Å is rather low). However, its peculiar emission-line properties, with some detectable low-ionization lines (Balmer lines, Mg II, Fe II), but very weak or no detectable higher ionization lines, are characteristic of other WLQ (Leighly et al. 2007a; Diamond-Stanic et al. 2009; Hryniewicz et al. 2010; Plotkin et al. 2010b; Shemmer et al. 2010; Wu et al. 2011). In the case of PHL 1811, this line emission is modelled by an unusually soft ionizing spectrum (Leighly et al. 2007b), which is however qualitatively similar to the emission of a cold AD. The soft ionizing SED produces little heating per ionization, and thus weak collisionally excited lines compared to recombination lines.

Some WLQ may be driven by different processes. The C IV EW is tightly inversely related with l (Baskin & Laor 2004) and also with other emission-line properties, such as the [O III] and Fe II EW (Baskin & Laor 2005), which are part of the eigenvector 1 correlations of various emission-line properties (Boroson & Green 1992). The C IV EW is also related to the C IV line peak velocity shift and profile asymmetry (e.g. Baskin & Laor 2005; Richards et al. 2011), and α_{ox} (Baskin & Laor 2005; Wu et al. 2009). This large set of correlations suggests that local effects in the BLR (e.g. metallicity, kinematics) may control the EW of C IV, and possibly of other high-ionization UV lines. If the driving mechanism for WLQ is a filtered ionizing continuum which illuminates the BLR (e.g. Richards et al. 2011; Wu et al. 2011), then the effect on the BLR excitation may be similar to the effect of a cold AD. However, the trend of decreasing C IV EW with increasing l cannot be confused with the cold AD effect, as higher l implies a hotter AD SED, rather than a colder one.

4.5 The absence of AGN with very broad lines

The combination of M and $\dot{M}$, which produces a cold AD, can be transformed to a limit on the Hβ FWHM, with very weak L_{opt} dependence. The local BB AD may become cold at $v > 8000\,\mathrm{km\,s^{-1}}$ when $a_* = 0$, and at $v > 16\,000\,\mathrm{km\,s^{-1}}$ when $a_* = 0.998$. The lower limit on v can be higher by a factor of up to 2 due to the inclination dependence of the ionizing continuum and possible deviation of the disc emission from a local BB continuum. AGN do show a sharp drop in their number at $v \gtrsim 10\,000\,\mathrm{km\,s^{-1}}$ (e.g. Hao et al. 2005; Shen et al. 2008), and this drop is independent of luminosity (Shen et al. 2008, their fig. 3). Laor (2003) suggested that there may be a yet unknown physical mechanism which suppresses the BLR at $v > 25\,000\,\mathrm{km\,s^{-1}}$. The AD becoming too cold to ionize the BLR may provide a natural explanation for the observed luminosity-independent limiting v, beyond which broad lines are not seen.

How does the line emission of AGN with the broadest lines appear? Do such objects enter the WLQ regime? Such a systematic study is not available yet. However, very broad line objects tend to have a double-peaked emission profile, and the spectrum of the 'prototypical' such object, ARP 102B, shows strong Balmer and Mg II lines, strong low-ionization forbidden lines, and relatively weak higher ionization lines (Halpern et al. 1996). Only anecdotal information is available for a couple of more such objects (Storchi-Bergmann et al. 2005; Eracleous, Lewis & Flohic 2009), partly consistent with the results for ARP 102B. A systematic study is clearly required to explore whether very broad line AGN indeed have emission-line properties intermediate between normal AGN and WLQ.

What is the SED of very broad line quasars? Strateva et al. (2008) show the overall SED of five double-peaked Balmer lines AGN, with $v \sim 14\,000$–$20\,000\,\mathrm{km\,s^{-1}}$. Their optical–UV SED is generally consistent with the average AGN SED, but the FUV at $\lambda < 1000$ Å is not probed. The objects have a flatter α_{ox} than the average for quasars at a similar luminosity (see also Strateva et al. 2006). This may indicate indirectly that significant X-ray heating is required for generating the broad lines in these objects, as very broad line quasars with an average α_{ox} may be selected against due to their weaker line emission. The flatter α_{ox} may therefore compensate for a smaller contribution of the UV continuum, if their AD is indeed

colder. A systematic study of the FUV emission of very broad line AGN can test if their FUV is indeed steeper.

4.6 Continuum-based searches for lineless quasars

An alternative approach to test the cold AD scenario is to explore the emission-line properties of AGN where the SED indicates weak FUV emission. It is important to note that red quasars (e.g. Richards et al. 2003) are not suitable objects, as a cold AD produces a normal blue continuum at $\lambda > 3200$ Å. Red quasars are affected either by dust extinction or by some other modification of the continuum emission mechanism. Cold AD candidates can be found by looking for quasars with a blue near-UV (NUV) slope, $\alpha_{\lambda>3200\,\text{Å}} > -1$, and a red FUV slope, $\alpha_{\lambda<1000\,\text{Å}} < -2$, as seen in SDSS J094533.99+100950.1 (Fig. 2). Such observation cannot be achieved from the ground, as the required $z > 3$ to probe the FUV slope from the ground leads to a high probability for an intervening Lyman limit absorption system ($\mathrm{d}n/\mathrm{d}z > 2$). Space-based UV observations of $z < 2$ quasars are essential for that, as was done by Hryniewicz et al. (2010) using *GALEX*.

The observed optical–UV SED of optically selected quasars shows a small dispersion (Elvis et al. 1994; Richards et al. 2006). Due to this Davis & Laor (2011) deduced that the accretion efficiency, η, increases with M, to compensate for the drop in the FUV with increasing M for AD models at a fixed η. One may worry that the implied rise in η with M is just a selection effect, as high M and low η quasars necessarily have a cold AD, produce weak line emission, and are selected against in a broad emission-line AGN survey. However, a colour-based AGN survey is not blind to a cold AD quasar, and as noted above, Diamond-Stanic et al. (2009) find that only 1.3 per cent of $z < 4.2$ colour-selected AGN are WLQ. Thus, there is no large population of low-a_* high-M quasars, and the high mean η (high a_*) values for high-M AGN deduced by Davis & Laor (2011) is not driven by emission-line selection.

We note that quasars generally show a soft-excess X-ray emission below 1 keV, compared to the 2–10 keV power-law emission (Wilkes & Elvis 1987), which may extend as a single power-law component to the FUV (Laor et al. 1997). This component is commonly attributed to Comptonization in a warm surface layer above the AD (e.g. Kriss et al. 1999). Such a layer can turn a cold AD SED into an ionizing SED. The SED of SDSS J094533.99+100950.1 is consistent with the exponential cold AD FUV cut-off, and shows no indication for a power-law component. Such a warm Comptonizing surface corona may be lacking in a cold AD (Czerny et al. 2011).

4.7 Cold AD in blazars

Ghisellini et al. (2009, 2010) attribute the optical–UV emission feature in blazars observed with the *Swift* satellite to thermal AD emission, based on the low polarization and low variability of this component. This component shows a peak in the NUV and a steep fall-off in the FUV, and is fitted with an AD model with very high values of M, up to $4 \times 10^{10}\,\mathrm{M}_\odot$ in some objects. These are therefore generally cold AD models, and if the BLR emission in these objects is powered mostly by the unbeamed thermal disc emission, some of these blazars should appear as WLQ. Indeed, some of the objects in Ghisellini et al. (2010) do show weaker UV lines (e.g. S5 0014+81, see Kuhr et al. 1983; Sargent, Steidel & Boksenberg 1989; PKS 2149−306, see Wilkes 1986; RBS 315, see Ellison et al. 2008), which may provide independent support for the cold AD interpretation of their optical–UV bump. However, intervening Lyman limit absorption systems are clearly contributing to the observed FUV steep fall-off in these $z \sim 2.5$–3.5 blazars, so the intrinsic AD continuum may not be as cold as observed. In addition, one cannot exclude additional line excitation from the highly luminous jets in these objects.

5 CONCLUSIONS

Standard thin AD models imply a non-ionizing continuum for high $M(\gtrsim 3 \times 10^9\,\mathrm{M}_\odot)$, even for fairly luminous quasars ($L_{\rm opt} = 10^{46}\,\mathrm{erg\,s^{-1}}$), in particular if the BH is non-rotating. Such cold AD may reside in AGN where the Balmer line FWHM > 8000–24 000 $\mathrm{km\,s^{-1}}$. The ionizing continuum in such objects originates only in the X-ray power-law component, which will likely produce an extended partially ionized region in the illuminated gas, which cools mostly through low-ionization lines. If $L_{\rm x} \lesssim 0.1 L_{\rm bol}$, as commonly seen in luminous AGN, the ionizing luminosity will be weaker by a factor of $\gtrsim 5$ than in average AGN. Such objects will appear as WLQ. If $L_{\rm x} \ll L_{\rm bol}$ such quasars may be lineless.

Cold ADs provide a natural explanation for the sharp drop in the number of AGN with broad line FWHM $\gtrsim 10\,000\,\mathrm{km\,s^{-1}}$, which is independent of luminosity. Follow-up FUV observations are required to test if very broad line AGN show the expected spectral turnover in the FUV, if they are powered by a cold AD. The best strategy is to obtain UV spectra of $z \sim 1$–2 very broad line quasars, to minimize the likelihood of intervening Lyman limit absorption by the intergalactic medium, or to detect such absorption if it occurs.

Colour-selected AGN samples indicate that only a small fraction (<6 per cent) of luminous AGN may harbour a cold AD. This can result from the high mean η values for AGN at high M, which may imply a higher a_* and a hotter AD emission which produces a higher $f_{\rm ion}$.

Searches for quasars with a blue optical–NUV and a red FUV continuum, using ground-based optical spectra, and space-based UV spectra of $1 < z \lesssim 2$ quasars, may be an efficient mechanism to reveal cold AD AGN. The continuum of a WLQ provided by Hryniewicz et al. (2010), which extends down to $\lambda = 570$ Å, is surprisingly well fitted by a simple local BB AD models. This is in contrast to most AGN, where the SED cannot be well fitted by a simple local BB AD model. The local BB models provide a better match than the TLUSTY-based models (Hubeny et al. 2000), suggesting that the effects of the Lyman edge and electron scattering opacity on the spectrum may be overestimated by these models.

Since both M and $L_{\rm opt}$ are determined from the observations of SDSS J094533.99+100950.1, only a_* and μ remain as free parameters to match the observed SED. The fit allows us to place an upper limit on the BH spin ($a_* \leq 0.3$) and a lower limit on the inclination of the AD ($\mu > 0.6$). The precise limits are somewhat uncertain, in part because the Mg II line-based estimates of M are uncertain. A larger M would allow a wider range of a_* and μ, but a smaller M would provide tighter constraints: an even lower limit on a_* and higher limit on μ, as further discussed by Czerny et al. (2011).

It is worthwhile to explore whether there are additional objects which can be well fitted by a cold AD SED, with only a_* and μ as free parameters. If such objects exist, the SED may provide a useful tool to constrain a_* and μ in such AGN, as commonly done in X-ray binaries. The AD fit may also provide some new insight on the structure of the AD atmosphere.

ACKNOWLEDGMENTS

We thank K. Hryniewicz for providing the data in electronic form. We thank Ohad Shemmer for useful discussions, and the referee

for useful comments. SWD is supported in part through NSERC of Canada.

REFERENCES

Anderson S. F. et al., 2001, AJ, 122, 503
Barger A. J., Cowie L. L., 2010, ApJ, 718, 1235
Baskin A., Laor A., 2004, MNRAS, 350, L31
Baskin A., Laor A., 2005, MNRAS, 356, 1029
Blackburne J. A., Pooley D., Rappaport S., Schechter P. L., 2011, ApJ, 729, 34
Blaes O., Hubeny I., Agol E., Krolik J. H., 2001, ApJ, 563, 560
Bonning E. W., Cheng L., Shields G. A., Salviander S., Gebhardt K., 2007, ApJ, 659, 211
Boroson T. A., Green R. F., 1992, ApJS, 80, 109
Czerny B., Elvis M., 1987, ApJ, 321, 305
Czerny B., Rózańska A., Kuraszkiewicz J., 2004, A&A, 428, 39
Czerny B., Hryniewicz K., Nikolajuk M., Sadowski A., 2011, MNRAS, 415, 2942
Davis S. W., Hubeny I., 2006, ApJS, 164, 530
Davis S. W., Laor A., 2011, ApJ, 728, 98
Davis S. W., Done C., Blaes O. M., 2006, ApJ, 647, 525
Davis S. W., Woo J.-H., Blaes O. M., 2007, ApJ, 668, 682
Diamond-Stanic A. M. et al., 2009, ApJ, 699, 782
Elitzur M., Ho L. C., 2009, ApJ, 701, L91
Elitzur M., Shlosman I., 2006, ApJ, 648, L101
Ellison S. L., York B. A., Pettini M., Kanekar N., 2008, MNRAS, 388, 1349
Elvis M. et al., 1994, ApJS, 95, 1
Eracleous M., Lewis K. T., Flohic H. M. L. G., 2009, New Astron., 53, 133
Eracleous M., Hwang J. A., Flohic H. M. L. G., 2010a, ApJS, 187, 135
Eracleous M., Hwang J. A., Flohic H. M. L. G., 2010b, ApJ, 711, 796
Fan X. et al., 1999, ApJ, 526, L57
Fan X. et al., 2006, AJ, 131, 1203
Ferland G. J., Netzer H., 1983, ApJ, 264, 105
Ganguly R. et al., 2007, AJ, 133, 479
Ghisellini G., Foschini L., Volonteri M., Ghirlanda G., Haardt F., Burlon D., Tavecchio F., 2009, MNRAS, 399, L24
Ghisellini G. et al., 2010, MNRAS, 405, 387
Hall P. B. et al., 2002, ApJS, 141, 267
Hall P. B. et al., 2004, AJ, 127, 3146
Halpern J. P., Eracleous M., Filippenko A. V., Chen K., 1996, ApJ, 464, 704
Hao L. et al., 2005, AJ, 129, 1783
Ho L. C., 2008, ARA&A, 46, 475
Hryniewicz K., Czerny B., Nikołajuk M., Kuraszkiewicz J., 2010, MNRAS, 404, 2028
Hubeny I., Agol E., Blaes O., Krolik J. H., 2000, ApJ, 533, 710
Janknecht E., Baade R., Reimers D., 2002, A&A, 391, L11
Just D. W., Brandt W. N., Shemmer O., Steffen A. T., Schneider D. P., Chartas G., Garmire G. P., 2007, ApJ, 665, 1004
Kaspi S., Smith P. S., Netzer H., Maoz D., Jannuzi B. T., Giveon U., 2000, ApJ, 533, 631
Kishimoto M., Antonucci R., Boisson C., Blaes O., 2004, MNRAS, 354, 1065
Kishimoto M., Antonucci R., Blaes O., Lawrence A., Boisson C., Albrecht M., Leipski C., 2008, Nat, 454, 492
Koratkar A., Blaes O., 1999, PASP, 111, 1
Kriss G. A., Davidsen A. F., Zheng W., Lee G., 1999, ApJ, 527, 683
Kuhr H., Liebert J. W., Strittmatter P. A., Schmidt G. D., Mackay C., 1983, ApJ, 275, L33
Kulkarni A. K. et al., 2011, MNRAS, 414, 1183
Laor A., 1990, MNRAS, 246, 369
Laor A., 2003, ApJ, 590, 86
Laor A., Netzer H., 1989, MNRAS, 238, 897
Laor A., Fiore F., Elvis M., Wilkes B. J., McDowell J. C., 1997, ApJ, 477, 93
Lawrence A., 2005, MNRAS, 363, 57
Leighly K. M., Halpern J. P., Jenkins E. B., Grupe D., Choi J., Prescott K. B., 2007a, ApJ, 663, 103
Leighly K. M., Halpern J. P., Jenkins E. B., Casebeer D., 2007b, ApJS, 173, 1
McDowell J. C., Canizares C., Elvis M., Lawrence A., Markoff S., Mathur S., Wilkes B. J., 1995, ApJ, 450, 585
Maoz D., 2007, MNRAS, 377, 1696
Morgan C. W., Kochanek C. S., Morgan N. D., Falco E. E., 2010, ApJ, 712, 1129
Narayan R., Mahadevan R., Quataert E., 1998, Theory of Black Hole Accretion Disks. Cambridge Univ. Press, Cambridge
Nicastro F., 2000, ApJ, 530, L65
Nicastro F., Martocchia A., Matt G., 2003, ApJ, 589, L13
Noble S. C., Krolik J. H., Schnittman J. D., Hawley J. F., 2011, preprint (arXiv:1105.2825)
Novikov I. D., Thorne K. S., 1973, in Dewitt C., Dewitt B. S., eds, Black Holes (Les Astres Occlus). Gordon & Breach, New York, p. 343
Plotkin R. M. et al., 2010a, AJ, 139, 390
Plotkin R. M., Anderson S. F., Brandt W. N., Diamond-Stanic A. M., Fan X., MacLeod C. L., Schneider D. P., Shemmer O., 2010b, ApJ, 721, 562
Reimers D., Janknecht E., Fechner C., Agafonova I. I., Levshakov S. A., Lopez S., 2005, A&A, 435, 17
Remillard R. A., McClintock J. E., 2006, ARA&A, 44, 49
Richards G. T. et al., 2003, AJ, 126, 1131
Richards G. T. et al., 2006, ApJS, 166, 470
Richards G. T. et al., 2011, AJ, 141, 167
Riffert H., Herold H., 1995, ApJ, 450, 508
Sargent W. L. W., Steidel C. C., Boksenberg A., 1989, ApJS, 69, 703
Shakura N. I., Sunyaev R. A., 1973, A&A, 24, 337 (SS73)
Shang Z. et al., 2005, ApJ, 619, 41
Shemmer O., Brandt W. N., Anderson S. F., Diamond-Stanic A. M., Fan X., Richards G. T., Schneider D. P., Strauss M. A., 2009, ApJ, 696, 580
Shemmer O. et al., 2010, ApJ, 722, L152
Shen Y., Greene J. E., Strauss M. A., Richards G. T., Schneider D. P., 2008, ApJ, 680, 169
Shi Y., Rieke G. H., Smith P., Rigby J., Hines D., Donley J., Schmidt G., Diamond-Stanic A. M., 2010, ApJ, 714, 115
Shields G. A., 1978, Nat, 272, 706
Songaila A., Cowie L. L., 2010, ApJ, 721, 1448
Storchi-Bergmann T., Nemmen R. S., Spinelli P. F., Eracleous M., Wilson A. S., Filippenko A. V., Livio M., 2005, ApJ, 624, L13
Strateva I. V., Brandt W. N., Eracleous M., Schneider D. P., Chartas G., 2006, ApJ, 651, 749
Strateva I. V., Brandt W. N., Eracleous M., Garmire G., 2008, ApJ, 687, 869
Sun W.-H., Malkan M. A., 1989, ApJ, 346, 68
Telfer R. C., Zheng W., Kriss G. A., Davidsen A. F., 2002, ApJ, 565, 773
Tran H. D., 2003, ApJ, 583, 632
Trump J. R. et al., 2011, ApJ, 733, 60
Wilkes B. J., 1986, MNRAS, 218, 331
Wilkes B. J., Elvis M., 1987, ApJ, 323, 243
Wu J., Vanden Berk D. E., Brandt W. N., Schneider D. P., Gibson R. R., Wu J., 2009, ApJ, 702, 767
Wu J. et al., 2011, ApJ, 736, 28
Zheng W., Kriss G. A., Telfer R. C., Grimes J. P., Davidsen A. F., 1997, ApJ, 475, 469

This paper has been typeset from a TEX/LATEX file prepared by the author.